



Hydroxychloroquine Induces Apoptosis in Cholangiocarcinoma *via* Reactive Oxygen Species Accumulation Induced by Autophagy Inhibition

Jiaqi Chen¹, Qiaoya Pan¹, Yang Bai², Xuepeng Chen^{1*} and Yi Zhou^{1*}

¹Stomatology Hospital, School of Stomatology, Zhejiang University School of Medicine, Clinical Research Center for Oral Diseases of Zhejiang Province, Key Laboratory of Oral Biomedical Research of Zhejiang Province, Cancer Center of Zhejiang University, Hangzhou, China, ²Department of Surgery, The Second Affiliated Hospital, Zhejiang University School of Medicine, Hangzhou, China

OPEN ACCESS

Edited by:

Bechan Sharma,
Allahabad University, India

Reviewed by:

Anna Atlante,
National Research Council (CNR), Italy
Valeria De Pasquale,
University of Naples Federico II, Italy
Tongsen Zheng,
Harbin Medical University Cancer
Hospital, China

*Correspondence:

Yi Zhou
zyuthscsa@zju.edu.cn
Xuepeng Chen
cxp1979@zju.edu.cn

Specialty section:

This article was submitted to
Cellular Biochemistry,
a section of the journal
Frontiers in Molecular Biosciences

Received: 04 June 2021

Accepted: 16 August 2021

Published: 10 September 2021

Citation:

Chen J, Pan Q, Bai Y, Chen X and
Zhou Y (2021) Hydroxychloroquine
Induces Apoptosis in
Cholangiocarcinoma *via* Reactive
Oxygen Species Accumulation
Induced by Autophagy Inhibition.
Front. Mol. Biosci. 8:720370.
doi: 10.3389/fmolb.2021.720370

Purpose: Despite considerable efforts to improve treatment modalities for cholangiocarcinoma, a common form of malignant tumor, its long-term survival rate remains poor. Hydroxychloroquine (HCQ) is a 4-aminoquinoline derivative antimalarial drug that has antimalarial and autophagy inhibition effects and exhibits comprehensive therapeutic effects on various cancers. In this study, we aimed to explore the anticancer potential and the underlying molecular mechanism of HCQ in cholangiocarcinoma treatment *in vitro* and *in vivo*.

Methods: Autophagy-related genes (ARGs) were obtained from the Human Autophagy Database and Molecular Signatures Database, and the expression profiles of ARGs were downloaded from the database of The Cancer Genome Atlas. Different expression gene sets were performed using R software. The Gene Ontology and KEGG enrichment analyses were performed to reveal significantly enriched signaling pathways and to identify differentially expressed genes in cholangiocarcinoma tissues. HuCCT-1 and CCLP-1 cells were exposed to different concentrations of HCQ. Cell proliferation was detected by Cell Counting Kit-8 (CCK-8), colony formation, and 5-ethynyl-2'-deoxyuridine (EdU) assays. Cell apoptosis and cycle arrest were detected by the Live/Dead cell assay and flow cytometry (FCM). The inhibition of autophagy was observed using fluorescence microscopy. The reactive oxygen species levels were assessed by fluorescence microscopy and flow cytometry. The protein levels were determined by western blot. A cholangiocarcinoma cell line xenograft model was used to evaluate the antitumor activity of HCQ *in vivo*.

Abbreviations: ARGs, autophagy-related genes; CCK-8, Cell Counting Kit-8; DCF, 2',7'-dichlorofluorescein; DE-ARGs, differential expression of autophagy-related gene sets; EdU, 5-ethynyl-2'-deoxyuridine; FCM, flow cytometry; FITC, fluorescein isothiocyanate isomer; GO, Gene Ontology; GSH, reduced L-glutathione; HCQ, hydroxychloroquine; IC50, half maximal inhibitory concentration; KEGG, Kyoto Encyclopedia of Genes and Genomes; LC3B, microtubule-associated proteins light chain 3B; PI, propidium iodide; ROS, reactive oxygen species; TCGA, The Cancer Genome Atlas; WB, western blotting.

Results: Compared with normal tissues, there were 141 ARGs with an aberrant expression in cholangiocarcinoma tissues which were mainly enriched in autophagy-related processes. Inhibition of autophagy by HCQ effectively suppressed cholangiocarcinoma *in vitro* and *in vivo*. HCQ inhibited cell proliferation and induced apoptosis and cycle arrest *in vitro* by increasing ROS accumulation, which was involved in autophagy inhibition. The ROS scavenger reduced L-glutathione distinctly weakened HCQ-induced cell apoptosis and viability inhibition in cholangiocarcinoma cells. In addition, HCQ inhibited growth of cholangiocarcinoma cell line xenograft tumors.

Conclusion: HCQ could inhibit cell proliferation and induce apoptosis in cholangiocarcinoma by triggering ROS accumulation *via* autophagy inhibition, which makes HCQ a potential antitumor drug candidate for cholangiocarcinoma treatment.

Keywords: HCQ, cholangiocarcinoma, ROS, autophagy, TCGA

INTRODUCTION

Cholangiocarcinoma is a malignant carcinoma that originates from the bile duct epithelium, which is characterized by the hidden onset and atypical early symptoms (Bekaii-Saab et al., 2021). Therefore, most patients are already in advanced stage when they are diagnosed for the first time, which leads to poor prognosis (O'Rourke et al., 2021). The main therapy for cholangiocarcinoma patients is surgical treatment (Rizvi et al., 2018). However, only a small percentage of patients can undergo radical surgery, and the postoperative local recurrence and distant metastasis rates remain very high (Blechacz, 2017). Given this, new therapeutic methods such as targeted therapy and immunotherapy are gradually being developed to improve patients' prognosis (Saeed et al., 2019). However, it is unfortunate that the treatment effect of cholangiocarcinoma remains unsatisfactory. Therefore, it is imperative to identify new strategies for the treatment of patients with cholangiocarcinoma.

Autophagy is an important type of programmed cell death, which involves the breakdown and the recycling of aging proteins as well as the damaged organelles such as mitochondria within cells (Onorati et al., 2018; Amaravadi et al., 2019; Xia et al., 2021). The reactive oxygen species (ROS) are accumulated when the mitochondrial membrane is damaged. Therefore, they in turn induce autophagy so as to promote the progress of advanced cancer (Chude and Amaravadi, 2017; Shi et al., 2017). As crucial modulators for cellular homeostasis, both of them are associated with the survival of tumor cells (Vera-Ramirez et al., 2018). Thus, targeting the autophagy progression by a non-specific inhibitor hydroxychloroquine (HCQ) in cholangiocarcinoma may supply new approaches for cancer prevention (Piao et al., 2017; Xu et al., 2018).

In recent years, autophagy-related gene (ARG) expression signatures have been used to construct a prognosis risk model in many types of tumors (Hu et al., 2020; Zhang et al., 2020). To our knowledge, ARGs were closely related to tumor prognosis (Shi et al., 2020). Here in this study, we performed a biological information analysis on the transcriptome information of The Cancer Genome Atlas (TCGA)-CHOL cohort to screen out the

differentially expressed ARGs. Meanwhile, we investigated the anticancer activities of HCQ in cholangiocarcinoma as well as the underlying molecular mechanisms of the process, which could support previous evidence on the role of autophagy in the development of cholangiocarcinoma and the potential therapeutic effect of other autophagy inhibitors (i.e., chloroquine, 3-methyladenine, wortmannin) (Yothaisong et al., 2013; Perez-Montoyo, 2020; Lendvai et al., 2021).

MATERIALS AND METHODS

Acquisition of Gene Expression Information and Autophagy-Related Gene Sets

Information of gene expression was downloaded from the TCGA-CHOL cohort database. ARGs were obtained from the Human Autophagy Database (HADDB). Finally, 44 mRNA expression profiles and 232 ARGs were obtained.

Identification of Differential Expression of Autophagy-Related Gene Sets and Enrichment Analysis

The “edgeR” package of R 4.0.3 software was used to analyze the differential expression of autophagy-related gene sets (DE-ARGs) in 35 cholangiocarcinoma samples and 9 normal samples. Gene Ontology (GO) functional enrichment and Kyoto Encyclopedia of Genes and Genomes (KEGG) signaling pathways were analyzed using the “clusterProfiler,” “ggplot2,” “org.HS.eg.db,” and “enrichplot” package of R 4.0.3 software.

Materials

The materials used in this study are hydroxychloroquine sulfate (cat. no. H141480, Aladdin), primary antibodies against caspase 3 (cat. no. ab184787, Abcam), PARP1 (cat. no. ab191217 Abcam), GAPDH (cat. no. ab181602, Abcam), cyclin E2 (cat. no. 4132, Cell Signaling Technology), p21 Waf1/Cip1 (12D1) (cat. no. 2947, Cell Signaling Technology), p53 (cat. no. ab26), Beclin-1 (cat. no. ab210498, Abcam), SQSTM1/p62 (cat. no. ab56416, Abcam), LC3B (cat. no. ab192890, Abcam), and LC3B (cat. no.

AF4650, Affinity), horseradish peroxidase-conjugated Goat Anti-Rabbit IgG (H + L) (cat. no. SA00001-2, Proteintech), horseradish peroxidase-conjugated Goat Anti-Mouse IgG (H + L) (cat. no. SA00001-1, Proteintech), and Alexa Fluor-conjugated Goat Anti-Rabbit IgG (H + L) (cat. no. ab150077, Abcam). The above antibodies were used at the recommended concentrations according to the manufacturer's instructions.

Cell Culture

Two human cholangiocarcinoma cell lines HuCCT-1 and CCLP-1 purchased from the American Type Culture Collection (Manassas, VA, United States) were cultured in RPMI 1640 medium (cat. no. 01-100-1A, Biological Industries) supplemented with 10% FBS (cat. no. 04-001-1B, Biological Industries) and incubated at 37°C and 5% CO₂.

Cell Counting Kit-8 Assay

For concentration-dependent cell viability experiments, HuCCT-1 and CCLP-1 cells were seeded into 96-well plates (4×10^3 cells/well) 18 h (37°C; 5% CO₂) prior to treatment with various concentrations (0, 30, 60, 90, 120, 150, 180, 210, 240, and 270 μmol/L) of HCQ for an additional 24 h (37°C; 5% CO₂). A total of 10 μL Cell Counting Kit-8 (CCK-8, cat. no. C0037, Beyotime) was subsequently added into each well for an additional 1.5 h (37°C; 5% CO₂), and the absorption value was measured using a spectrophotometer. For time-dependent cell viability experiments, the cells were plated into 96-well plates 18 h (37°C; 5% CO₂) prior to treatment with the IC₅₀ and 2*IC₅₀ concentrations of HCQ for 0, 6, 12, 24, 48, and 72 h (37°C; 5% CO₂), and the optical density was measured at different time points in the same way. Curves were fitted and analyzed using GraphPad Prism 8 software (GraphPad Software, Inc.).

Colony Formation Assay

HuCCT-1 and CCLP-1 cells were digested, counted, and seeded in a six-well plate (Guangzhou Jet Bio-Filtration Co., Ltd., 3,000–5,000 cells per well) 18 h prior to treatment with the IC₅₀ and 2*IC₅₀ concentrations of HCQ for 24 h. For the L-glutathione-reduced (GSH) group, the cells were preincubated with GSH (3 mmol/L) for 2 h and then treated with HCQ for 24 h. Then, the cells were cultured for another few days and stained with crystal violet. A clone was defined as more than 50 cells.

EdU Viability Assay

According to the manufacturer's instructions, the Cell Light EdU Apollo 567 *in vitro* kit (Guangzhou RiboBio Co., Ltd.) was used to evaluate the effect of HCQ. After treatment with IC₅₀ and 2*IC₅₀ concentrations of HCQ for 24 h, HuCCT-1 and CCLP-1 cells were EdU labeled and incubated for 2 h. Then, Apollo and Hoechst 33342 staining was performed. Fluorescence microscopy (Olympus Corporation, Japan) was used to photograph the cells.

Cell Apoptosis and Cell Cycle Analysis

Apoptosis was determined by an Annexin V-FITC Apoptosis Detection Kit (cat. no. C1062L, Beyotime). HuCCT-1 and CCLP-1 cells were seeded at a density of 4×10^5 cells per well in

six-well plates. Following exposure to IC₅₀ and 2*IC₅₀ concentrations of HCQ for 24 h, the cells were incubated with Annexin V-FITC (fluorescein isothiocyanate isomer) and propidium iodine (PI) for 20 min at 37°C in the dark according to the manufacturer's protocol. For the GSH group, the cells were preincubated with GSH (3 mmol/L) for 2 h and then treated with HCQ for 24 h. Cell cycle distribution was determined by a Cell Cycle and Apoptosis Analysis Kit (cat. no. C1052, Beyotime). Following exposure to the IC₅₀ concentration of HCQ for 24 h, the cells were collected and fixed with 75% precooled ethanol. Upon completion of treatment, the cells were stained with PI for 20 min according to the instructions. Finally, apoptosis and cell cycle distribution were examined by flow cytometry (FCM, BD Biosciences, United States) and analyzed by Flowjo software 10.6.2 (FlowJo LLC) and ModFit LT software 5 (Verity Software House, Inc.).

Live/Dead Cell Assay

Live/Dead cells were determined by a Calcein/PI Cell Viability/Cytotoxicity Assay Kit (cat. no. C2015M, Beyotime). Following exposure to IC₅₀ and 2*IC₅₀ concentrations of HCQ for 24 h, HuCCT-1 and CCLP-1 cells were digested and stained with Calcein-AM and PI for 30 min at room temperature. Pictures were taken using a fluorescence microscope (Olympus IX71).

Reactive Oxygen Species Detection

The accumulation of ROS was detected by an ROS assay kit (cat. no. S0033S, Beyotime). The cells were exposed to HCQ for 24 h. For the GSH group, the cells were preincubated with GSH (3 mmol/L) for 2 h and then treated with HCQ for 24 h. Then, the cells were collected and incubated with 10 μmol/L 2,7-dichlorodihydrofluorescein diacetate (DCFH-DA) at 37°C for 30 min and washed three times. The level of ROS was determined by fluorescence microscopy and FCM.

Immunofluorescence Microscopy

After treatment with the IC₅₀ concentration of HCQ for 24 h, HuCCT-1 and CCLP-1 cells were subsequently incubated with rabbit polyclonal antibody against LC3B (1:400) overnight at 4°C. Following addition of fluorochrome-conjugated anti-rabbit IgG (1:200) and incubation at 37°C for 1 h, DAPI counterstaining was performed at room temperature for 30 min. Pictures were taken using an Olympus IX71 digital camera.

Autophagy Flux Detection

The cells were seeded in a confocal dish at a density of 10,000 cells per dish. Following exposure to adenovirus expressing mCherry-GFP-LC3B fusion protein recognizing CD46 (AdPlus-mCherry-GFP-LC3B, cat. no. C3012, Beyotime) for 48 h, the cells were incubated with the IC₅₀ concentration of HCQ for 24 h. Pictures were taken using ZEISS LSM 900 confocal microscopy.

Western Blot Analysis

Western blot analysis was performed as reported previously (Wang et al., 2021). HuCCT-1 and CCLP-1 cells were digested and dissolved in Radio Immunoprecipitation Assay (RIPA) Lysis Buffer (cat. no. P0013B, Beyotime) containing 1% protease inhibitor cocktail (cat. no. P8340, Sigma-Aldrich) for 1 h. An

enhanced BCA Protein Assay Kit (cat. no. P0010, Beyotime) was then used to detect the protein concentration. Equal amounts of protein were then separated on 10% SurePAGE Bis-Tris gels (cat. no. M00664, GenScript) for electrophoresis and transferred to polyvinylidene fluoride (PVDF) membranes. Membranes were then blocked using a QuickBlock Blocking Buffer (cat. no. P0252, Beyotime) at 37°C for 1 h and incubated with primary antibodies against GAPDH, caspase 3, PARP1, cyclin E2, p21, p53, Beclin-1, LC3B, and SQSTM1/P62 at 1:1,000 overnight. Membranes were then incubated with anti-rabbit secondary antibodies at 1:2,500 for 1 h at room temperature, and protein bands were finally detected by an Enhanced Chemiluminescence Kit (cat. no. G2014, Servicebio). Band intensity was quantified using ImageJ software (National Institutes of Health).

In Vivo Tumor Xenograft Models

Ten BALB/c nude mice (5 weeks old, 18–20 g) were housed under specific-pathogen-free (SPF) conditions. Approximately 5×10^6 CCLP-1 cells were injected into the right back of each mouse subcutaneously to establish the tumor model. Until the tumors reached about 100 mm (Rizvi et al., 2018), the mice were randomly assigned into two groups: 1) control group ($n = 5$, 0.9% physiological saline) and 2) HCQ group ($n = 5$, 100 mg/kg). These compounds were administered intraperitoneally once daily. The body weight and tumor size were recorded during the treated period. The mice were sacrificed 3 weeks after injection.

Immunohistochemistry Staining

The immunohistochemistry of the xenograft tumor was conducted as previously described (Cao et al., 2020). 2 mm thick sections were stained with hematoxylin and eosin (HE) for the analysis of inflammation and necrosis. Tumor tissues were subjected to immunohistochemical staining of Ki-67 for the analysis of proliferation ability. Apoptotic cells were determined by TdT-mediated dUTP nick-end labeling (TUNEL) technique with a TUNEL Apoptosis Assay Kit (cat. no. C1091, Beyotime) following the manufacturer's instructions.

Statistical Analysis

Data and figures were processed using GraphPad Prism 8 software (GraphPad Software, Inc.). All values were expressed as mean \pm standard deviation (SD) and assessed using Student's *t*-test or one-way analysis of variance procedure. Except for the *in vivo* tumor xenograft experiment (five mice were allocated to each group, so as to ensure the sufficient group size for statistical analysis) which was carried out only once, all other experiments were carried out in triplicate with at least three independent experiments. $p < 0.05$ was considered to indicate a statistically significant difference.

RESULTS

Identification and Enrichment Analysis of DE-ARGs

In this work, mRNA expression profiles with 35 cholangiocarcinoma samples and 9 normal samples were

collected from the TCGA database, and 232 ARGs were obtained from the HADB. The heat map of DE-ARGs in cholangiocarcinoma is shown in **Supplementary Figure 1A**. Compared with the normal tissues, there were 141 DE-ARGs in cholangiocarcinoma tissues which contained 138 up-regulated ARGs and only 3 down-regulated ARGs (**Figures 1A,B**). GO functional enrichment analysis showed that DE-ARGs were mostly enriched in autophagy and phagophore assembly sites to perform the functions of biological processes and cell components, respectively (**Figures 1C,D**). Moreover, KEGG signaling pathway analysis showed that DE-ARGs mostly enriched in some programmed cell death signaling pathways such as autophagy and apoptosis (**Supplementary Figures 1B,C**). These results suggested that autophagy might play a crucial role in the development of cholangiocarcinoma, and the inhibition of it might have therapeutic effect on cholangiocarcinoma.

Inhibition of Autophagy Reduced the Activity of Cholangiocarcinoma Cells

The above results confirmed that the autophagy process was active in cholangiocarcinoma tissues, so we hypothesized that inhibition of autophagy could have a therapeutic effect on tumors. The classic autophagy inhibitor HCQ was selected to treat two cholangiocarcinoma cell lines, HuCCT-1 and CCLP-1. As shown in **Figure 2A**, the cell viability of HuCCT-1 and CCLP-1 cells was significantly inhibited by HCQ, and the IC₅₀ of the two cell lines was $168.4 \pm 23.4 \mu\text{mol/L}$ and $113.36 \pm 14.06 \mu\text{mol/L}$, respectively. Moreover, cholangiocarcinoma cells were inhibited by HCQ in a time-dependent manner (**Supplementary Figures 2A,B**). The colony formation assay and EdU assay also indicated that the colony formation ability (for the IC₅₀ group, $p < 0.01$ in HuCCT-1 and $p < 0.05$ in CCLP-1) and the proliferation ability ($p < 0.01$) of cholangiocarcinoma cells were significantly inhibited in HCQ-treated cells (**Figures 2B,C, Supplementary Figures 2C,D**).

HCQ Induced Apoptosis in Cholangiocarcinoma Cells

Cell death can significantly affect cell viability. After the treatment with IC₅₀ and 2*IC₅₀ concentrations of HCQ for 24 h, FCM with FITC/PI double staining was used to confirm the role of HCQ in inducing apoptosis in cholangiocarcinoma cells. Compared with the control group, apoptosis in the HuCCT-1 and CCLP-1 cells (for the IC₅₀ group, $p < 0.001$ in HuCCT-1 and $p < 0.01$ in CCLP-1) increased in a dose-dependent manner after the 24 h HCQ treatment (**Figure 3A, Supplementary Figures 3A,B**). Consistent with the FCM results, the Live/Dead cell assay revealed a significant transition from the calcein signal to the PI signal (**Figure 3B**), indicating that HCQ-induced apoptosis increased with the increase of dose. To further determine whether apoptosis occurred instead of necrosis or other forms of cell death, we used western blotting (WB) to explore the expression of caspase 3 and PARP1, which were both downstream apoptosis-related proteins. As shown in

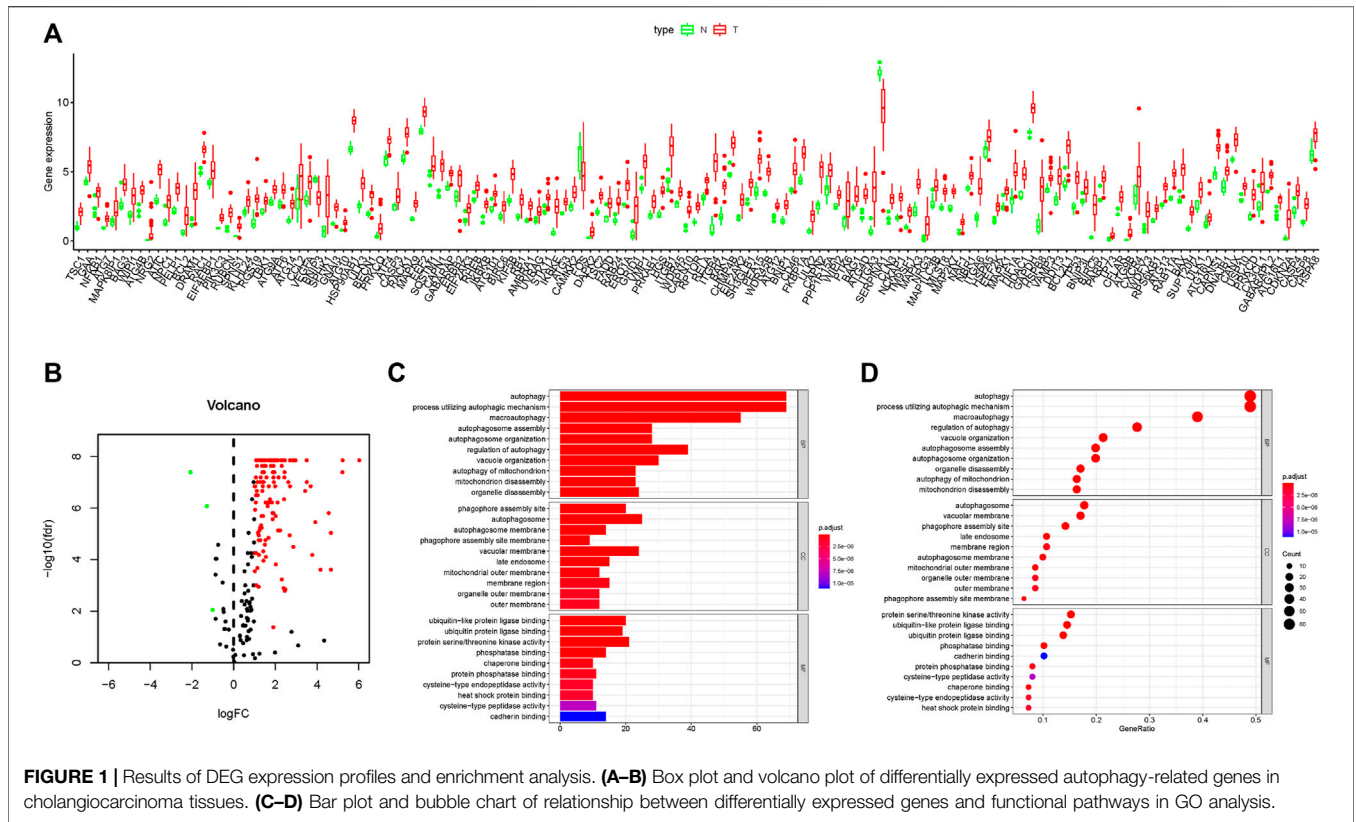


FIGURE 1 | Results of DEG expression profiles and enrichment analysis. **(A–B)** Box plot and volcano plot of differentially expressed autophagy-related genes in cholangiocarcinoma tissues. **(C–D)** Bar plot and bubble chart of relationship between differentially expressed genes and functional pathways in GO analysis.

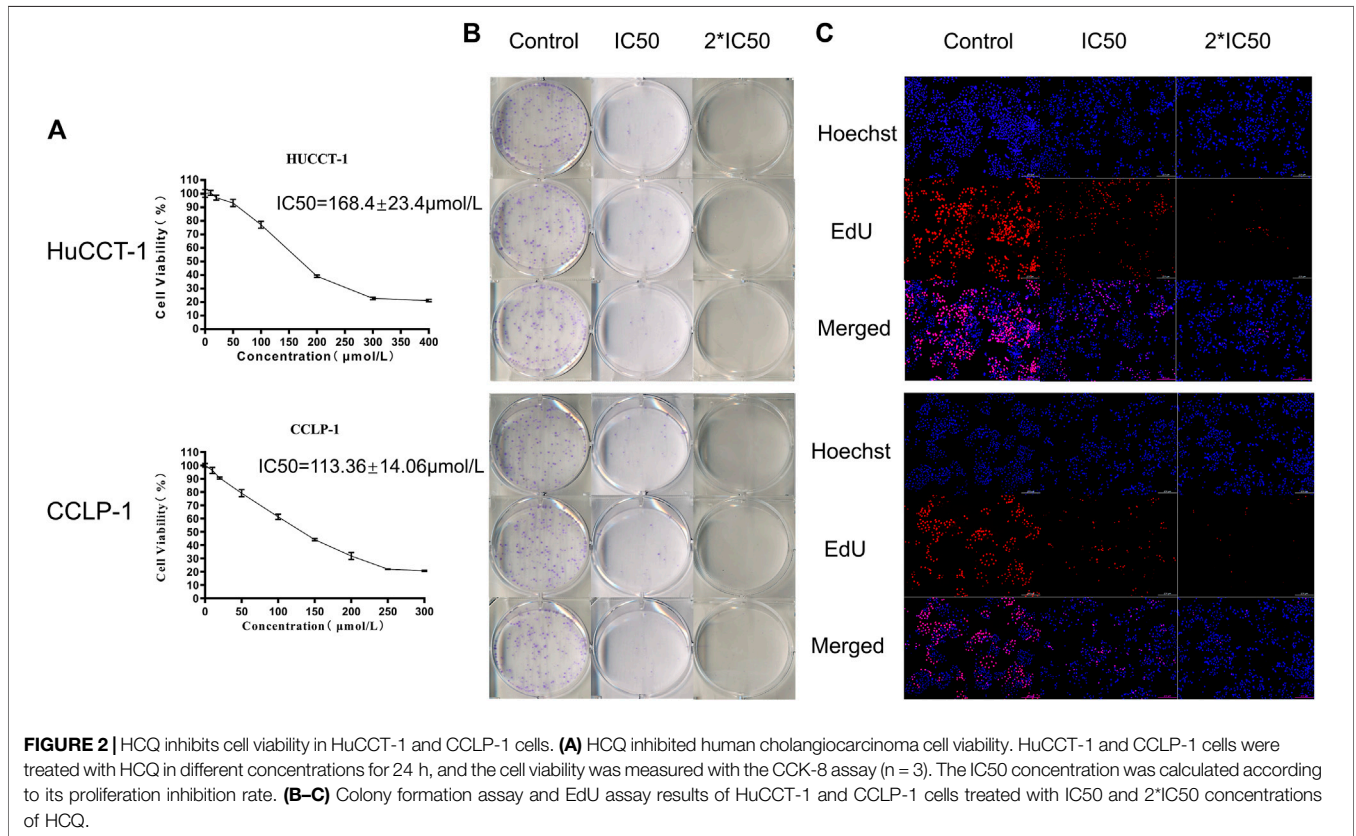
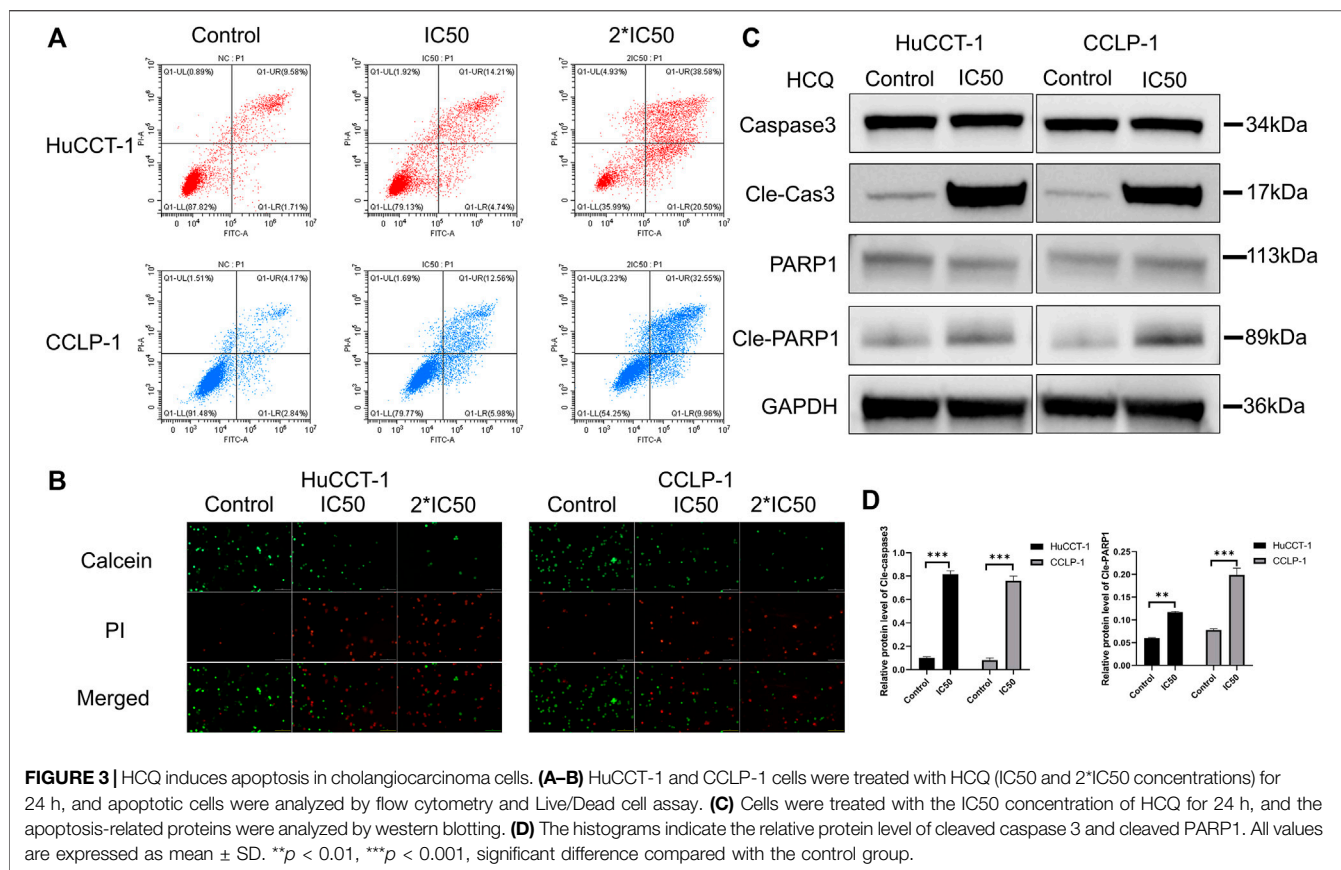


FIGURE 2 | HCQ inhibits cell viability in HuCCT-1 and CCLP-1 cells. **(A)** HCQ inhibited human cholangiocarcinoma cell viability. HuCCT-1 and CCLP-1 cells were treated with HCQ in different concentrations for 24 h, and the cell viability was measured with the CCK-8 assay ($n = 3$). The IC50 concentration was calculated according to its proliferation inhibition rate. **(B–C)** Colony formation assay and EdU assay results of HuCCT-1 and CCLP-1 cells treated with IC50 and 2*IC50 concentrations of HCQ.



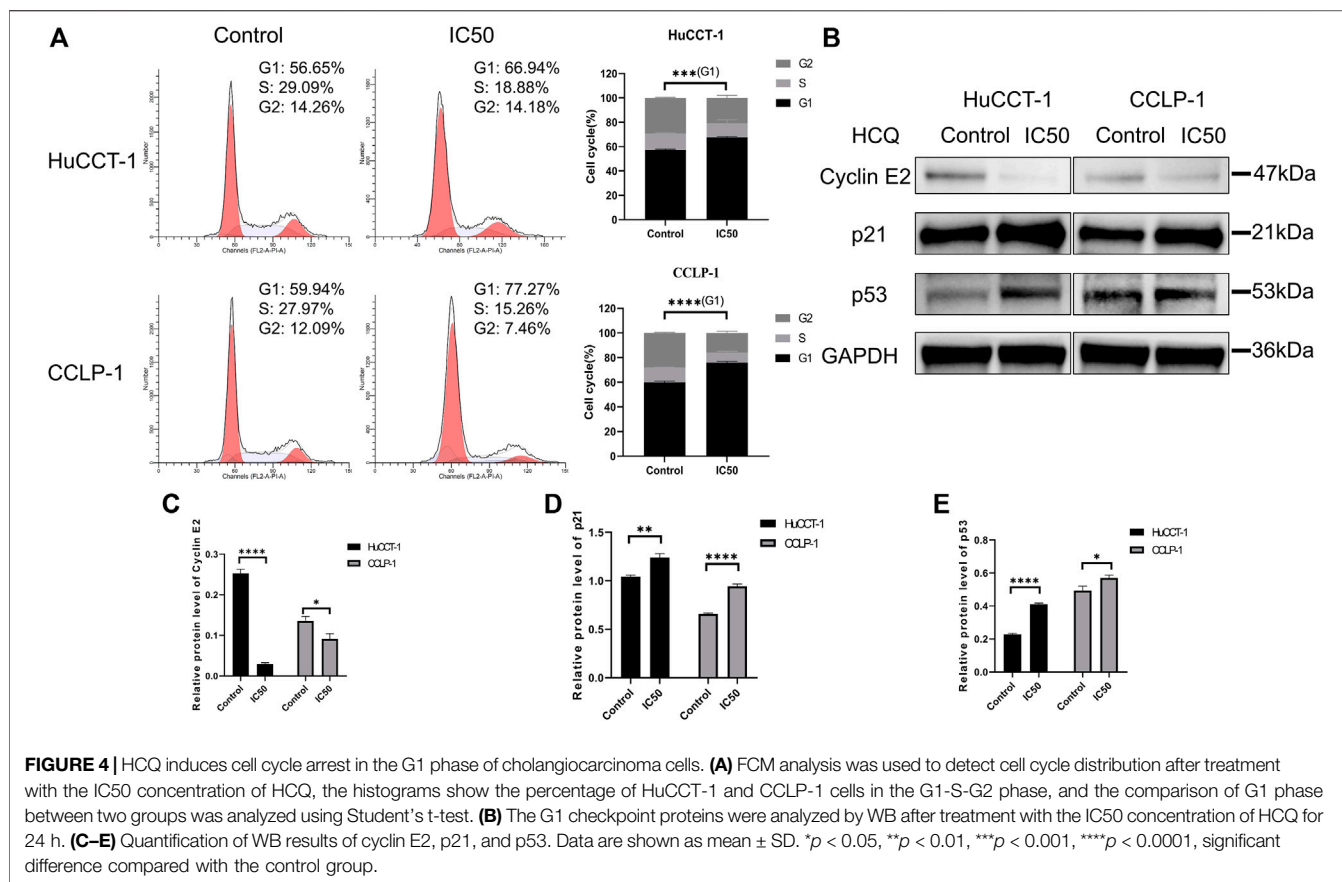
Figures 3C,D, the expression of cleaved caspase 3 ($p < 0.001$) and cleaved PARP1 ($p < 0.01$ in HuCCCT-1 and $p < 0.001$ in CCLP-1) increased significantly, while the expression of caspase 3 and PARP1 had no significant change. In brief, these data suggested that HCQ induced cholangiocarcinoma cell death by activating apoptosis pathways.

HCQ Induced G1 Arrest in Cholangiocarcinoma Cells

To determine the underlying mechanism resulting in the suppression of cell proliferation and loss of cell viability, cell cycle distribution was assessed using FCM. As shown in **Figure 4A**, an increase in the percentage of cells in G1 phase was observed in HuCCCT-1 and CCLP-1 cells after being treated with the IC50 concentration of HCQ for 24 h, from 56.65 to 66.94% ($p < 0.001$) and from 59.94 to 77.27% ($p < 0.0001$), respectively. Next, the expression of the G1 checkpoint protein was detected using WB. As presented in **Figures 4B–E**, p21 ($p < 0.01$ in HuCCCT-1 and $p < 0.0001$ in CCLP-1) and p53 ($p < 0.0001$ in HuCCCT-1 and $p < 0.05$ in CCLP-1) increased markedly, and a marked reduction was observed in cyclin E2 ($p < 0.0001$ in HuCCCT-1 and $p < 0.05$ in CCLP-1), which indicated that treatment of HCQ with IC50 concentration might result in G1 arrest in cholangiocarcinoma cells.

HCQ Induced ROS Accumulation by Inhibiting Autophagy

HCQ may inhibit autophagy to decrease the elimination of damaged organelles so as to increase the excessive production of ROS in cholangiocarcinoma cells. Autophagy inhibition and ROS content were analyzed using immunofluorescence (IF) microscopy and FCM. As shown in **Figure 5A**, microtubule-associated proteins light chain 3B (LC3B)-positive punctate dots (green fluorescence) increased markedly after HCQ (IC50) treatment in HuCCCT-1 and CCLP-1 cells. After the treatment with the IC50 concentration of HCQ for 24 h, mCherry-GFP-LC3B was aggregated on the membrane of autophagosome in the form of yellow spots under a confocal microscope which means autophagy inhibition (**Figure 5B**). Correspondingly, the mean fluorescence intensity of 2',7'-dichlorofluorescein (DCF) increased significantly after HCQ treatment in both cell types (**Figure 5C**, **Supplementary Figures 4A,B**, $p < 0.0001$ in HuCCCT-1 and $p < 0.01$ in CCLP-1), suggesting that ROS had accumulated. When autophagy was inhibited, the degradation of LC3-II and sequestosome 1/P62 (SQSTM1/P62) was reduced, while the process of LC3 conversion from LC3-I to LC3-II and SQSTM1/P62 synthesis continued. Therefore, autophagy was assessed using the content of SQSTM1/P62 and the LC3-II/LC3-I ratio by WB analysis. In **Figures 5D,E**, following HCQ (IC50 and 2*IC50) treatment, LC3B-II ($p < 0.01$) and SQSTM1/



P62 ($p < 0.01$) increased markedly in both cell types, while Beclin-1 did not reveal any significant change.

HCQ-Mediated Apoptosis of Cholangiocarcinoma Cells Occurred in an ROS-Dependent Manner

HCQ can induce apoptosis of cholangiocarcinoma and ROS accumulation. Therefore, we hypothesized that HCQ disrupted cholangiocarcinoma survival by inducing alterations in ROS levels. Subsequently, we examined the effects of L-glutathione-reduced (GSH) group, which scavenged ROS, on colony formation and apoptosis. As shown in **Figure 6A** and **Supplementary Figure 5A**, the increase of ROS levels in HuCCT-1 and CCLP-1 cells was reversed by GSH treatment (for the HCQ + GSH group, $p < 0.01$ in HuCCT-1 and $p < 0.001$ in CCLP-1). Colony formation and apoptosis analysis had produced similar results. The effect of HCQ on inhibition of cholangiocarcinoma cells was reversed by GSH treatment (**Figures 6B,C, Supplementary Figure 5B**). At the protein level, the increase in cleaved caspase 3 (for the HCQ + GSH group, $p < 0.01$ in HuCCT-1 and no significant change in CCLP-1) and cleaved PARP1 (for the HCQ + GSH group, $p < 0.001$ in HuCCT-1 and $p < 0.05$ in CCLP-1) in HuCCT-1 and CCLP-1 cells was reversed by HCQ treatment (**Figures 6D,E**). Collectively, our results

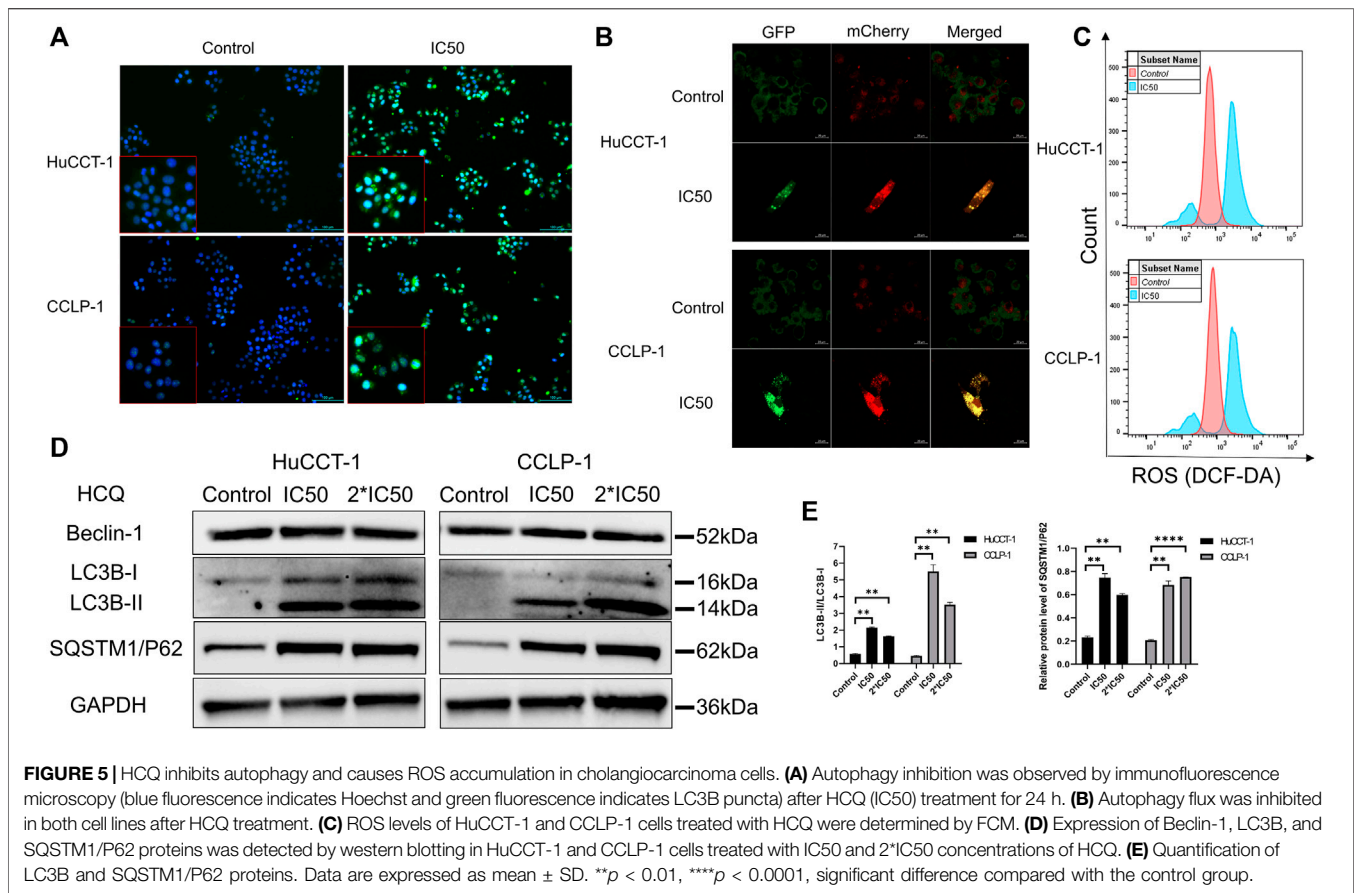
demonstrated that GSH decreased ROS levels, which in turn reversed survival of cholangiocarcinoma cells.

HCQ Suppressed *In Vivo* Growth of Tumors

To investigate the effect of HCQ on tumor growth *in vivo*, mice bearing cholangiocarcinoma subcutaneous xenografts were used. As shown in **Figures 7A,B**, we found that tumor weight was significantly reduced following HCQ treatment for 3 weeks. From the seventh day after HCQ administration, the growth rate of the tumor was significantly reduced compared to that observed in the control group, while there was no significant difference in body weight of mice between two groups (**Figure 7C, Supplementary Figure 5C**). IHC analysis revealed a dramatic reduction of Ki-67 staining and significantly increase of TUNEL staining in the tumor tissues of mice treated with HCQ (**Figure 7D**) which meant that the proliferation of cholangiocarcinoma was inhibited and apoptosis played a huge role in it. In summary, our results suggested that HCQ inhibited cholangiocarcinoma growth *in vivo*.

DISCUSSION

Nowadays, several prognostic factors are identified to determine cholangiocarcinoma prognosis, including the ceRNA regulatory network (Xia et al., 2020) and DNA methylation (Nakaoka et al.,

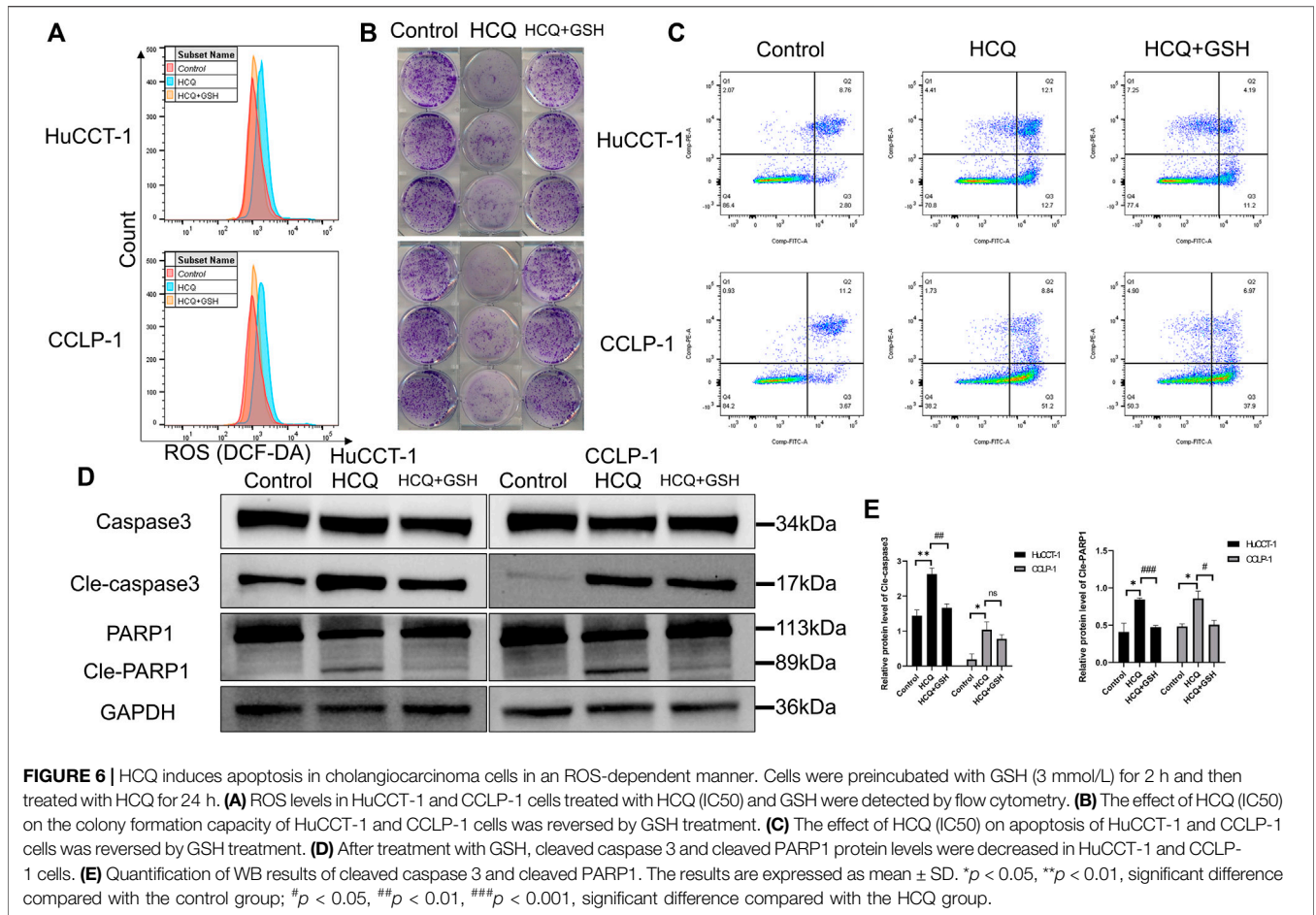


2017). Meanwhile, high-throughput sequencing datasets (Jeon et al., 2018) or several effective biomarkers (Lang et al., 2021) are being used to explore potential molecular mechanisms in cholangiocarcinoma treatment. Due to its comprehensive genetic heterogeneity, the key drivers involved in the genesis and development of cholangiocarcinoma still need to be defined. Autophagy maintains cellular homeostasis by degrading defective organelles, which is an evolutionarily conserved process (Eskelinen, 2019). Autophagy can also prevent the buildup of misfolded proteins and the development of ROS. It means the inhibition of autophagy may result in autophagic cell death (Liang et al., 2020). In this study, we focused on the genetic changes in the transcription level to discover DE-ARGs between cholangiocarcinoma tissues and normal tissues. The vast majority of ARGs were up-regulated in cholangiocarcinoma, which inhibited autophagy to suppress cell proliferation and induced apoptosis in cholangiocarcinoma by triggering ROS accumulation.

Most advanced tumors exist in a circumstance with hypoxia and insufficient energy. In order to adapt to the environment, tumor tissues usually activate autophagy to maintain their high metabolic rate. Therefore, ARGs are often differentially expressed in tumor tissues and normal tissues. Fang and Chen (2020) reported that, among 487 autophagy-related genes in hepatocellular carcinoma, 60 differentially expressed genes had more than twice expression fold difference. Wang et al. (2019) reported that more than 30% of ARGs

were differentially expressed in gliomas, and enrichment analysis showed that the biological process (BP) of these DE-ARGs was related to the assembly of autophagosomes. Thongchot et al. (2021) found that the expression of MAP1LC3B (LC3B, an autophagy marker gene) was up-regulated in cholangiocarcinoma and the two-year overall survival rate of patients with high expression of LC3B was higher than that of patients with low expression of LC3B from the survival curve, although there was no significant difference ($p = 0.3761$) in five-year overall survival between the two groups. As can be seen from our results, most ARGs were up-regulated in cholangiocarcinoma and the main BP was enriched in the assembly of autophagosomes. These results made it possible for us to use HCQ in the treatment of cholangiocarcinoma for the function of autophagy inhibition by HCQ that comes from the fusion suppression of autophagosomes and lysosomes (Hazari et al., 2020).

The effect of HCQ is similar to that of chloroquine, but its toxicity is only half that of chloroquine. They are used to treat tumors, initially as adjuvant drugs in combination with other antitumor drugs (Maycotte et al., 2012; Dragowska et al., 2013). It has been reported that chloroquine can enhance the antitumor effect of epirubicin. The combination of the two drugs can reduce the cell viability of lung cancer cells by about 20% and significantly increase the apoptosis of lung cancer cells (Liang et al., 2020). In addition, chloroquine can also enhance the treatment effect of some potential antitumor peptide on

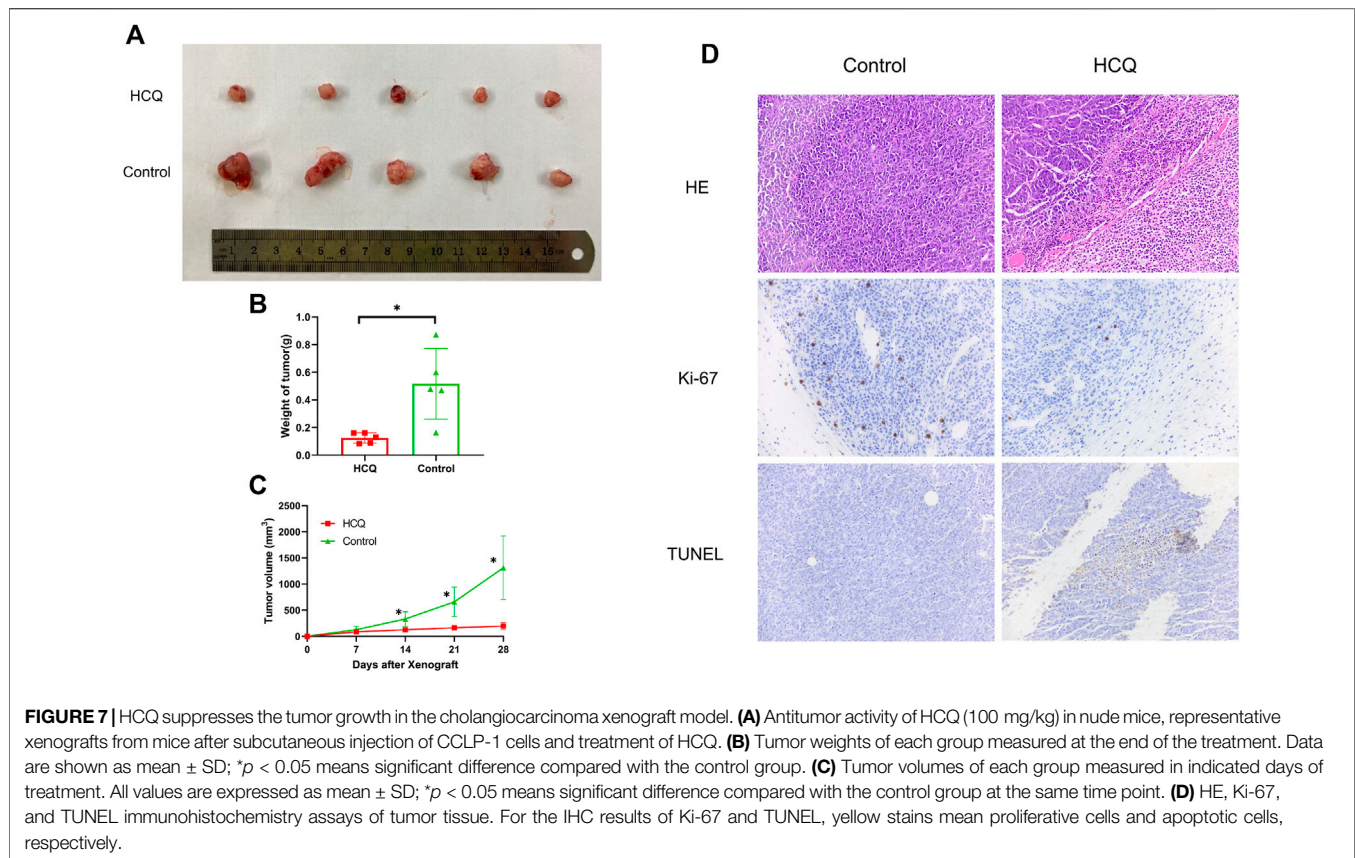


cervical cancer which may be related to the inhibition of autophagy. With the deepening of research, some scholars found that chloroquine or HCQ could not only be used as adjuvant drugs to treat tumors but also produce good antitumor effects as a single agent. For non-small-cell lung cancer and pancreatic cancer, the IC50 concentrations of HCQ *in vitro* were 65 $\mu\text{mol/L}$ and 33 $\mu\text{mol/L}$, respectively (Nordström et al., 2015). This value was $168.4 \pm 23.4 \mu\text{mol/L}$ and $113.36 \pm 14.06 \mu\text{mol/L}$ in HuCCT-1 and CCLP-1 cholangiocarcinoma cells according to our results, respectively, which meant that HCQ could also be extremely effective in cholangiocarcinoma treatment. When the IC50 concentration of HCQ was used for cholangiocarcinoma administration, we confirmed that the number of apoptotic cells and the expression of apoptosis-related proteins (cleaved caspase 3 and cleaved PARP1) increased significantly, accompanied by G1 phase arrest. These results implied that cell apoptosis and cycle arrest might be involved in the inhibitory effect of HCQ on cholangiocarcinoma.

The main mechanism of HCQ is to inhibit the membrane fusion of autophagosomes and lysosomes, so as to play a repression role in the final stage of autophagy (Klionsky et al., 2016; Mauthe et al., 2018). mCherry is a monomeric red fluorescent protein from mushroom coral. During the fusion of autophagosomes and lysosomes, the acidic environment within the lysosome causes the

green fluorescent protein (GFP) to be quenched. When mCherry and GFP were used to label the LC3B protein together, the fluorescence in the cell will excite different colors of fluorescence depending on the autophagy state. The results from our study clearly indicated that cholangiocarcinoma cells in the control group showed scattered red spots under the background of diffuse yellow fluorescence (combined effect of mCherry and GFP) in the cytoplasm. We considered the possible reason was that when autophagosomes fused with lysosomes, the green fluorescence of GFP was partially quenched and the red fluorescence was displayed. When cholangiocarcinoma cells underwent apoptosis (IC50 concentration), the fusion of autophagosomes and lysosomes was inhibited by HCQ, while autophagy proceeded smoothly upstream. And therefore, mCherry-GFP-LC3B was aggregated on the membrane of autophagosome in the form of yellow spots under a confocal microscope. Meanwhile, the results of western blot also verified an increasing expression of autophagy-related proteins.

ROS in cells is mainly produced by electrons leaking from the mitochondrial electron transport chain (Zussman et al., 2020). It will produce a series of toxic and side effects on various cell membrane structures in cells, resulting in cell death (Hayes et al., 2020). Zhu et al. (2020) reported that administration of 20 $\mu\text{mol/L}$ irinotecan for 24 h could significantly increase the ROS content in gastric cancer cells and result in apoptosis of gastric cancer cells



with the help of autophagy. Other drugs (heteronemin, etc.) could also induce ROS to produce similar killing effect on cholangiocarcinoma cells (Thongsom et al., 2017; Chang et al., 2021). Similarly, HCQ induced apoptosis of cholangiocarcinoma cells with an up-regulation of ROS from our data. We suspected that necrotic and aging organelles could not be removed after autophagy was inhibited, therefore resulting in more ROS production. When GSH (a scavenger of ROS) was added, apoptosis was reduced to a certain extent, which might imply that ROS have a certain killing effect on tumor cells act as the downstream of autophagy.

Although our experiments have verified the antitumor effect of HCQ at the cellular and animal levels, our work still has some shortcomings, which are mainly reflected in animal experiments. Our results revealed that HCQ showed a good therapeutic effect on animals, but we did not further explore the detailed mechanism of HCQ *in vivo*. Considering the complexity of pharmacokinetics *in vivo* (Chen et al., 2018), we believe that the antitumor effect of HCQ *in vivo* should have its similarities and differences compared with that *in vitro*. This will be the direction we need to strive for in the future.

CONCLUSION

In summary, our study indicated that HCQ induced autophagy-dependent apoptosis in cholangiocarcinoma cells *via* ROS

accumulation, which could support previous evidence on the role of autophagy in the development of cholangiocarcinoma and provide some novel insights into the mechanism of the autophagy inhibitor HCQ.

DATA AVAILABILITY STATEMENT

The original contributions presented in the study are included in the article/Supplementary Material, further inquiries can be directed to the corresponding authors.

ETHICS STATEMENT

The animal study was reviewed and approved by the Experimental Animal Welfare Ethics Committee of Zhejiang Laboratory Animal Center.

AUTHOR CONTRIBUTIONS

YZ and XC conceived and designed the study. JC and YB conducted the study. JC and QP contributed to the acquisition of data. JC and YB analyzed and interpreted the data. YZ and XC reviewed and edited the article. All authors read and gave final approval of the article.

FUNDING

This research was supported by the Zhejiang Provincial Natural Science Foundation of China under Grant No. LY18H140001.

REFERENCES

- Amaravadi, R., Kimmelman, A., and Debnath, J. (2019). Targeting Autophagy in Cancer: Recent Advances and Future Directions. *Cancer Discov.* 9 (9), 1167–1181. doi:10.1158/2159-8290.cd-19-0292
- Bekaii-Saab, T., Bridgewater, J., and Normanno, N. (2021). Practical Considerations in Screening for Genetic Alterations in Cholangiocarcinoma. *Ann. Oncol.* 32 (9), 1111–1126. doi:10.1016/j.annonc.2021.04.012
- Blechacz, B. (2017). Cholangiocarcinoma: Current Knowledge and New Developments. *Gut and liver* 11 (1), 13–26. doi:10.5009/gnl15568
- Cao, Y., Wang, J., Tian, H., and Fu, G. (2020). Mitochondrial ROS Accumulation Inhibiting JAK2/STAT3 Pathway Is a Critical Modulator of CYT997-Induced Autophagy and Apoptosis in Gastric Cancer. *J. Exp. Clin. Cancer Res. : CR* 39 (1), 119. doi:10.1186/s13046-020-01621-y
- Chang, W., Bow, Y., Fu, P., Li, C. Y., Wu, C. Y., Chang, Y. H., et al. (2021). A Marine Terpenoid, Heteronemin, Induces Both the Apoptosis and Ferroptosis of Hepatocellular Carcinoma Cells and Involves the ROS and MAPK Pathways. *Oxidative Med. Cell. longevity* 2021, 7689045. doi:10.1155/2021/7689045
- Chen, T., Cheng, Y., Huang, P., and Chen, P. (2018). Facilitated Unbinding via Multivalency-Enabled Ternary Complexes: New Paradigm for Protein-DNA Interactions. *Acc. Chem. Res.* 51 (4), 860–868. doi:10.1021/acs.accounts.7b00541
- Chude, C., and Amaravadi, R. (2017). Targeting Autophagy in Cancer: Update on Clinical Trials and Novel Inhibitors. *Int. J. Mol. Sci.* 18 (6), 1279. doi:10.3390/ijms18061279
- Dragowska, W., Weppler, S., Wang, J., Wong, L. Y., Kapanen, A. I., Rawji, J. S., et al. (2013). Induction of Autophagy Is an Early Response to Gefitinib and a Potential Therapeutic Target in Breast Cancer. *PLoS one* 8 (10), e76503. doi:10.1371/journal.pone.0076503
- Eskelinen, E. (2019). Autophagy: Supporting Cellular and Organismal Homeostasis by Self-Eating. *Int. J. Biochem. Cel. Biol.* 111, 1–10. doi:10.1016/j.biocel.2019.03.010
- Fang, Q., and Chen, H. (2020). Development of a Novel Autophagy-Related Prognostic Signature and Nomogram for Hepatocellular Carcinoma. *Front. Oncol.* 10, 591356. doi:10.3389/fonc.2020.591356
- Hayes, J., Dinkova-Kostova, A., and Tew, K. (2020). Oxidative Stress in Cancer. *Cancer cell* 38 (2), 167–197. doi:10.1016/j.ccell.2020.06.001
- Hazari, Y., Bravo-San Pedro, J., Hetz, C., Galluzzi, L., and Kroemer, G. (2020). Autophagy in Hepatic Adaptation to Stress. *J. Hepatol.* 72 (1), 183–196. doi:10.1016/j.jhep.2019.08.026
- Hu, D., Jiang, L., Luo, S., Zhao, X., Hu, H., Zhao, G., et al. (2020). Development of an Autophagy-Related Gene Expression Signature for Prognosis Prediction in Prostate Cancer Patients. *J. translational Med.* 18 (1), 160. doi:10.1186/s12967-020-02323-x
- Jeon, J., Maeng, L., Bae, Y., Lee, E., Yoon, Y., and Yoon, N. (2018). Comparing Clonality between Components of Combined Hepatocellular Carcinoma and Cholangiocarcinoma by Targeted Sequencing. *Cancer genomics & proteomics* 15 (4), 291–298. doi:10.21873/cgp.20087
- Klionsky, D., Abdelmohsen, K., Abe, A., Abedin, M. J., Abeliovich, H., Acevedo Arozena, A., et al. (2016). Guidelines for the Use and Interpretation of Assays for Monitoring Autophagy (3rd Edition). *Autophagy* 12 (1), 1–222. doi:10.1080/15548627.2015.1100356
- Lang, S., Bednarsch, J., Joechle, K., Amygdalos, I., Czigan, Z., Heij, L., et al. (2021). Prognostic Biomarkers for Cholangiocarcinoma (CCA): State of the Art. *Expert Rev. Gastroenterol. Hepatol.* 15 (5), 1–14. doi:10.1080/17474124.2021.1912591
- Lendvai, G., Szekerczés, T., Illyés, I., Csengeri, M., Schlachter, K., Szabó, E., et al. (2021). Autophagy Activity in Cholangiocarcinoma Is Associated with Anatomical Localization of the Tumor. *PLoS one* 16 (6), e0253065. doi:10.1371/journal.pone.0253065

SUPPLEMENTARY MATERIAL

The Supplementary Material for this article can be found online at: <https://www.frontiersin.org/articles/10.3389/fmolb.2021.720370/full#supplementary-material>

- Liang, A., Zhang, J., Du, S., Zhang, B., Ma, X., Wu, C. Y., et al. (2020). Chloroquine Increases the Anti-cancer Activity of Epirubicin in A549 Lung Cancer Cells. *Oncol. Lett.* 20 (1), 53–60. doi:10.3892/ol.2020.11567
- Liang, S., Li, X., Gao, C., and Zhang, L. (2020). microRNA-based Autophagy Inhibition as Targeted Therapy in Pancreatic Cancer. *Biomed. Pharmacother. = Biomedicine pharmacotherapie* 132, 110799. doi:10.1016/j.biopha.2020.110799
- Mauthe, M., Orhon, I., Rocchi, C., Zhou, X., Luhr, M., Hijlkema, K. J., et al. (2018). Chloroquine Inhibits Autophagic Flux by Decreasing Autophagosomal-Lysosomal Fusion. *Autophagy* 14 (8), 1435–1455. doi:10.1080/15548627.2018.1474314
- Maycotte, P., Aryal, S., Cummings, C., Thorburn, J., Morgan, M., and Thorburn, A. (2012). Chloroquine Sensitizes Breast Cancer Cells to Chemotherapy Independent of Autophagy. *Autophagy* 8 (2), 200–212. doi:10.4161/auto.8.2.18554
- Nakaoka, T., Saito, Y., and Saito, H. (2017). Aberrant DNA Methylation as a Biomarker and a Therapeutic Target of Cholangiocarcinoma. *Int. J. Mol. Sci.* 18 (6), 1111. doi:10.3390/ijms18061111
- Nordström, L., Sironi, J., Aranda, E., Maisonet, J., Perez-Soler, R., Wu, P., et al. (2015). Discovery of Autophagy Inhibitors with Antiproliferative Activity in Lung and Pancreatic Cancer Cells. *ACS Med. Chem. Lett.* 6 (2), 134–139.
- O'Rourke, C., Munoz-Garrido, P., and Andersen, J. (2021). Molecular Targets in Cholangiocarcinoma. *Hepatology* 73, 62–74. doi:10.1002/hep.31278
- Onorati, A., Dyczynski, M., Ojha, R., and Amaravadi, R. (2018). Targeting Autophagy in Cancer. *Cancer* 124 (16), 3307–3318. doi:10.1002/cncr.31335
- Perez-Montoyo, H. (2020). Therapeutic Potential of Autophagy Modulation in Cholangiocarcinoma. *Cells* 9 (3), 614. doi:10.3390/cells9030614
- Piao, S., Ojha, R., Rebecca, V., Samanta, A., Ma, X. H., McAfee, Q., et al. (2017). ALDH1A1 and HLF Modulate the Activity of Lysosomal Autophagy Inhibitors in Cancer Cells. *Autophagy* 13 (12), 2056–2071. doi:10.1080/15548627.2017.1377377
- Rizvi, S., Khan, S. A., Hallemeier, C. L., Kelley, R. K., and Gores, G. J. (2018). Cholangiocarcinoma - Evolving Concepts and Therapeutic Strategies. *Nat. Rev. Clin. Oncol.* 15 (2), 95–111. doi:10.1038/nrclinonc.2017.157
- Saeed, A., Park, R., Al-Jumayli, M., Al-Rajabi, R., and Sun, W. (2019). Biologics, Immunotherapy, and Future Directions in the Treatment of Advanced Cholangiocarcinoma. *Clin. colorectal Cancer* 18 (2), 81–90. doi:10.1016/j.clcc.2019.02.005
- Shi, H., Zhong, F., Yi, X., Shi, Z., Ou, F., Xu, Z., et al. (2020). Application of an Autophagy-Related Gene Prognostic Risk Model Based on TCGA Database in Cervical Cancer. *Front. Genet.* 11, 616998. doi:10.3389/fgene.2020.616998
- Shi, T., Yu, X., Yan, L., and Xiao, H. (2017). Research Progress of Hydroxychloroquine and Autophagy Inhibitors on Cancer. *Cancer Chemother. Pharmacol.* 79 (2), 287–294. doi:10.1007/s00280-016-3197-1
- Thongchot, S., Vidoni, C., Ferraresi, A., Loilome, W., Khuntikeo, N., Sangkhamanon, S., et al. (2021). Cancer-Associated Fibroblast-Derived IL-6 Determines Unfavorable Prognosis in Cholangiocarcinoma by Affecting Autophagy-Associated Chemoresponse. *Cancers* 13 (9), 2134. doi:10.3390/cancers13092134
- Thongsom, S., Suginta, W., Lee, K., Choe, H., and Talabnin, C. (2017). Piperlongumine Induces G2/M Phase Arrest and Apoptosis in Cholangiocarcinoma Cells through the ROS-JNK-ERK Signaling Pathway. *Apoptosis : Int. J. programmed Cel. Death* 22 (11), 1473–1484. doi:10.1007/s10495-017-1422-y
- Vera-Ramirez, L., Vodnala, S., Nini, R., Hunter, K., and Green, J. (2018). Autophagy Promotes the Survival of Dormant Breast Cancer Cells and Metastatic Tumour Recurrence. *Nat. Commun.* 9 (1), 1944. doi:10.1038/s41467-018-04070-6
- Wang, F., Wang, L., Qu, C., Chen, L., Geng, Y., Cheng, C., et al. (2021). Kaempferol Induces ROS-dependent Apoptosis in Pancreatic Cancer Cells via TGM2-Mediated Akt/mTOR Signaling. *BMC cancer* 21 (1), 396. doi:10.1186/s12885-021-08158-z

- Wang, Z., Gao, L., Guo, X., Feng, C., Lian, W., Deng, K., et al. (2019). Development and Validation of a Nomogram with an Autophagy-Related Gene Signature for Predicting Survival in Patients with Glioblastoma. *Aging* 11 (24), 12246–12269. doi:10.18632/aging.102566
- Xia, H., Green, D., and Zou, W. (2021). Autophagy in Tumour Immunity and Therapy. *Nat. Rev. Cancer* 21 (5), 281–297. doi:10.1038/s41568-021-00344-2
- Xia, L., Chen, X., Yang, J., Zhu, S., Zhang, L., Yin, Q., et al. (2020). Long Non-coding RNA-PAICC Promotes the Tumorigenesis of Human Intrahepatic Cholangiocarcinoma by Increasing YAP1 Transcription. *Front. Oncol.* 10, 595533. doi:10.3389/fonc.2020.595533
- Xu, R., Ji, Z., Xu, C., and Zhu, J. (2018). The Clinical Value of Using Chloroquine or Hydroxychloroquine as Autophagy Inhibitors in the Treatment of Cancers: A Systematic Review and Meta-Analysis. *Medicine* 97 (46), e12912. doi:10.1097/md.00000000000012912
- Yothaisong, S., Dokduang, H., Techasen, A., Namwat, N., Yongvanit, P., Bhudhisawasdi, V., et al. (2013). Increased Activation of PI3K/AKT Signaling Pathway Is Associated with Cholangiocarcinoma Metastasis and PI3K/mTOR Inhibition Presents a Possible Therapeutic Strategy. *Tumour Biol.* 34 (6), 3637–3648. doi:10.1007/s13277-013-0945-2
- Zhang, J., Wang, Z., Zhao, R., An, L., Zhou, X., Zhao, Y., et al. (2020). An Integrated Autophagy-Related Gene Signature Predicts Prognosis in Human Endometrial Cancer. *BMC cancer* 20 (1), 1030. doi:10.1186/s12885-020-07535-4
- Zhu, Q., Guo, Y., Chen, S., Fu, D., Li, Y., Li, Z., et al. (2020). Irinotecan Induces Autophagy-dependent Apoptosis and Positively Regulates ROS-Related JNK- and P38-MAPK Pathways in Gastric Cancer Cells. *OncoTargets Ther.* 13, 2807–2817. doi:10.2147/ott.s240803
- Zussman, R., Xu, L., Damani, T., Groom, K. M., Chen, Q., Seers, B., et al. (2020). Antiphospholipid Antibodies Can Specifically Target Placental Mitochondria and Induce ROS Production. *J. Autoimmun.* 111, 102437. doi:10.1016/j.jaut.2020.102437

Conflict of Interest: The authors declare that the research was conducted in the absence of any commercial or financial relationships that could be construed as a potential conflict of interest.

Publisher's Note: All claims expressed in this article are solely those of the authors and do not necessarily represent those of their affiliated organizations, or those of the publisher, the editors, and the reviewers. Any product that may be evaluated in this article, or claim that may be made by its manufacturer, is not guaranteed or endorsed by the publisher.

Copyright © 2021 Chen, Pan, Bai, Chen and Zhou. This is an open-access article distributed under the terms of the Creative Commons Attribution License (CC BY). The use, distribution or reproduction in other forums is permitted, provided the original author(s) and the copyright owner(s) are credited and that the original publication in this journal is cited, in accordance with accepted academic practice. No use, distribution or reproduction is permitted which does not comply with these terms.